

New Evaluation Techniques for Gas Shale Reservoirs



*Rick Lewis, David Ingraham, Marc Percy: Oklahoma City
Jerome Williamson, Walt Sawyer, Joe Frantz: Pittsburgh*

ABSTRACT

The mature, organic-rich shales sourcing much of the hydrocarbons that have been produced from conventional reservoirs in the United States now represent both developed reserves and potential resources. Gas shales have become an attractive target because they represent a huge resource (500 to 780 TCF¹), and as the price of gas rises, the economic challenge of their development is reduced. Multiple operators are currently leasing and evaluating gas shale properties throughout the United States. If the prospective gas shales can be economically developed, many thousands of wells will be drilled in this region during the next decade.

Key reservoir parameters for gas shale deposits include: 1) thermal maturity, 2) reservoir thickness, 3) total organic carbon (TOC) content, 4) adsorbed gas fraction, 5) free gas fraction within the pores and fractures, and 6) permeability. The first two parameters are routinely measured. Thermal maturity is commonly measured in core analysis and reservoir thickness is routinely measured with logs. The calculation of the final four parameters requires a novel approach.

A robust gas shale interpretation package has been developed utilizing the Platform Express[®] and Elemental Capture Spectroscopy[®] (ECS) logging tools. The ECS is key to this package as it provides gamma-ray-independent clay content plus a matrix density that compensates for the variable lithology typical of gas shale. ELAN[®] Elemental Log Analysis is used to quantify kerogen and calculate porosity and gas saturations.

A complete gas shale log evaluation requires calibration to core for thermal maturity and a metric to equate TOC to adsorbed gas. The best data for the latter is a Langmuir isotherm that provides a characteristic gas pressure and volume measured at a specific temperature.

INTRODUCTION

Onshore United States represents a hyper-mature gas development play. Most conventional reservoirs have already been exploited. With the current high price for gas, more effort is being applied to the development of non-conventional gas plays: tight gas, coalbed methane, and shale gas.

Some of the earliest gas wells produced from shales; however, their low flow rates limited development interest. Recently, gas shales have become a more attractive target because they rep-

resent a huge resource (500 to 780 TCF¹) and the economic challenges for their development have lessened with rising gas prices and new evaluation and completion technologies.

Gas shales are complex reservoirs. They represent significant variety in reservoir characteristics (i.e., mineralogy, porosity, permeability, gas content, and pressure). The gas in shales occurs both as a free phase within pores and fractures and as gas sorbed onto organic matter. Gas shales generally have a porosity of 4 to 6 pu and a total organic carbon content (TOC) of 4 weight percent or greater².

Gas shales represent a unique reservoir due to their very low permeabilities. Most have a matrix permeability of 10⁻⁴ to 10⁻⁸ mD. The presence, density, and continuity of natural, open fractures are believed to be critical to enhance system permeability. Successful development generally entails hydraulic fracturing in order to connect these natural fractures to the wellbore.

Initial production in gas shales generally decreases rapidly to a fairly low rate that may persist for 20 years or longer. For this reason, large projects, with attendant economies of scale, have proven necessary to successfully develop these unconventional reservoirs. Gas shale has been an economic target since the 1980's, particularly in the Northeastern US where over 28,000 wells have been drilled as of 2000¹. Figure 1 shows currently producing gas shale fields and the extent of these gas shales.

Events over the last several years have dramatically increased industry interest in discovering and developing shale gas reservoirs. The greatest success has been with the Mississippi Barnett Shale in the Fort Worth Basin of Texas. The Barnett Shale East Newark Field has developed into the largest gas field in Texas with annual production in 2002 of approximately 200 BCF and proven gas reserves in excess of 3.5 TCF³. The Barnett Shale has an estimated gas in place greater than 120 BCF per square mile. Most encouraging has been the increase in estimated ultimate recovery (EUR) of the average Barnett well from 0.3 BCF before 1990 to 1.25 BCF in 2002⁴. The increase in EUR is due primarily to increase in gas recovery; current gas recovery is estimated to be 8 to 12%⁵. It is still low compared to conventional reservoirs, primarily because of low matrix permeability.

Many operators are currently leasing large acreage positions throughout the Mid-continent in search of the next Barnett-type play. They need accurate evaluation methodologies to evaluate their gas shale resource and predict production. This paper describes demonstrated solutions for these needs. If these

¹ Mark of Schlumberger

formations can be developed economically, many thousands of wells will be drilled in this region during the next decade.

APPROACH

Gas Shale Characteristics

Shale is the most common sedimentary rock. Shale with the potential to be an economic gas reservoir, in contrast, is relatively rare. Due to their low permeability, gas shales are self-sourced. They must have the requisite volume and type of organic matter and proper thermal history to generate hydrocarbons, especially gas. The first step in any evaluation is the identification of a potential gas shale reservoir.

Figure 2 is Platform Express log of a gas shale overlying a conventional shale. The upper shale (the Devonian-Mississippian Woodford Formation of Oklahoma which has generated 8% of the world's original petroleum reserves⁶) exhibits a typical gas shale log response with

- very high gamma ray activity
- high resistivity
- low bulk density
- low Pe.

This characteristic log response is a function of the high concentration of kerogen, the insoluble organic material within the shale. The petrophysical properties of kerogen are listed in Table 1. The best-constrained property is bulk density⁷, which ranges from 0.95 to 1.05 g/cm³. Kerogen creates a reducing environment that leads to the precipitation of uranium and resulting high gamma ray activity. Although diagnostic, the high gamma ray activity, is quite variable due to differences in pH, Eh, temperature, pressure, U⁶/U⁴ activities, and activities of other cations and anions⁸. Also, resistivity in gas shales is high due to low water saturations, usually irreducible, resulting from the expulsion of hydrocarbons.

Kerogen / TOC Quantification

The amount of sorbed gas is a function of kerogen content, pore pressure, and temperature. Quantifying the kerogen content, typically defined as TOC, is a necessary step in evaluating a shale gas. There are numerous papers on the use of conventional wireline logs to evaluate and quantify kerogen in shales, both as a source rock⁹ and as a potential reservoir¹⁰. Most conventional algorithms rely on either the density or sonic log to differentiate kerogen; thus, both require an accurate estimate of matrix properties. This may be difficult due to variable non-clay mineralogy within the gas shales (e.g., pyrite mineralization and calcite concretions). In addition, these schemes only provide kerogen content; they do not convert it to TOC or calculate adsorbed gas.

Another property of great interest is the clay mineral content of gas shales. Clay quantification can prove problematic in any shale due to the different types of clay minerals that may be present and variability in key petrophysical properties within clay types (e.g., gamma ray activity, neutron porosity, sonic slowness). Figure 3 is a cross-plot of gamma ray activity versus clay content for a gas shale exploratory test drilled in the Mid-Continent (all subsequent logs and modeling results in this paper are from this same well). There is a well-defined trend suggesting that clay content is a function of gamma ray activity, but there are

also data that do not adhere to this trend. These data represent the gas shale because their variable kerogen content is driving gamma ray activity.

An accurate predictor of clay content is Al¹¹. There are no logging tools fielded today that can precisely measure this element. One solution is SpectroLith*, a series of empirical relationships that provide an Al emulation based on the quantity of Si, Ca, and Fe¹¹ in the formation. SpectroLith calculates clay, carbonate, pyrite, and quartz-feldspar-mica weight percent.

The Elemental Capture Spectroscopy* (ECS) is a geochemical log that quantifies Si, Ca, Fe, Ti, S and Gd plus other elements. SpectroLith was developed expressly to maximize the benefit of this service. Kerogen is composed primarily of C, H, and O, elements that are not used by SpectroLith to calculate mineralogy. Thus, the geochemical log provides a clay estimate that does not rely on petrophysical parameters sensitive to kerogen content.

Figure 4 is a SpectroLith log of a conventional shale overlying a gas shale. Clay content was determined by XRD on sidewall core, and the results compare favorably. The gamma ray activity is over plotted, and it is apparent that gamma ray is not an accurate estimator of clay content within the gas shale. The clay content of the gas shale is actually lower than the conventional shale, a feature common to many gas shales. SpectroLith also indicates that the gas shale has variable quantities of pyrite and carbonate, in contrast to the overlying conventional shale.

Kerogen can be accurately estimated through the merging of a conventional triple combo log with a geochemical log. This merging also permits the calculation of an accurate mineralogy, including clay type and content, and an estimate of key petrophysical properties (porosity, saturation and permeability). A petrophysical interpretation program such as ELAN¹²⁻¹³ can be used to solve for these volumes. SpectroLith mineral volumes can be readily incorporated into ELAN¹⁴. (Kerogen should be assigned to the quartz-feldspar-mica volume.)

Figure 5 shows the inputs into the ELAN analysis (gamma ray, porosity, Pe, and SpectroLith), and the resulting ELAN volumes. Kerogen volume is readily distinguished through the gas shale interval. The figure also shows the ELAN parameters used for kerogen. Track 3 of this figure compares matrix density calculated from the geochemical log¹⁵ and from ELAN. Comparison to core analysis indicates that both matrix densities compare well in the conventional shale, but not in the gas shale. The matrix density from ELAN compares well with core because it solves for the low-density kerogen; the matrix density from the geochemical data is too high because these measurements are insensitive to the elements in kerogen.

Earlier generation openhole geochemical logging tools also measured C and O. It was possible to directly calculate kerogen with these additional elemental concentrations¹⁶. However, these tools are no longer available.

Once kerogen volume is estimated, the next step is to calculate the adsorbed gas volume. First, kerogen volume must be converted to TOC. The conversion is in the following equation¹⁶ (Equation 1). TOC does not account for other elements that may occur within kerogen (H, O, N, S), so a conversion factor is required that accounts for the missing elements and considers kerogen type and maturity. Table 2 lists these factors⁷; but 1.2 is generally a reasonable value.

$$TOC = \frac{\phi_{ker} \cdot \rho_{ker}}{\rho_b \cdot \kappa} \quad (1)$$

Where:

- TOC = total organic carbon (lbf/lbf)
 ϕ_{ker} = kerogen volume (vol/vol)
 ρ_{ker} = kerogen density (g/cm³)
 ρ_b = bulk density (g/cm³)
 κ = kerogen conversion factor

Track 2 of Figure 6 compares TOC calculated from logs with core.

Adsorbed Gas Quantification

Adsorbed gas, methane sorbed to the surface of kerogen, is in equilibrium with methane in gas phase. The Langmuir isotherm¹⁷ was developed to describe this type of equilibrium at a specific temperature (Equation 2). More complex isotherms have been calculated to define this equilibrium, but the Langmuir provides sufficient precision, and it is the industry standard. Core analysis is required to generate a Langmuir isotherm. However, generally only one Langmuir isotherm is necessary to adequately describe a gas shale within a field or sub-basin.

$$gc = \frac{V_l p}{(p + P_l)} \quad (2)$$

Where:

- gc = gas content (scf/ton)
 p = reservoir pressure (psia)
 V_l = Langmuir volume (scf/ton)
 P_l = Langmuir pressure (psia)

Examination of the equation shows that one must know the Langmuir volume and Langmuir pressure plus reservoir pressure. Figure 7 depicts a typical Langmuir isotherm where the curved line defines the equilibrium between adsorbed and free gas as a function of reservoir pressure at the isotherm temperature. The shape of this curve is defined by the Langmuir volume (volume of adsorbed gas at infinite pressure) and the Langmuir pressure (pressure where one-half of the gas at infinite pressure has been desorbed).

The Langmuir isotherm is measure at a specific TOC and temperature. Application to log evaluation should contain corrections to account for variability in these two parameters. A temperature correction is presented in Equations 3 to 6. The constants c3 and c7 were initially developed for coalbed methane¹⁶.

$$V_{lt} = 10^{(-c3 \cdot (T+c4))} \quad (3)$$

$$P_{lt} = 10^{(c7 \cdot (T+c8))} \quad (4)$$

$$c4 = \log V_l + (c3 \cdot T_i) \quad (5)$$

$$c8 = \log P_l + (-c7 \cdot T_i) \quad (6)$$

Where:

- V_{lt} = Langmuir volume at reservoir temp (scf/ton)
 P_{lt} = Langmuir pressure at reservoir temp (psia)
 $c3$ = 0.0027
 $c7$ = 0.005
 T = reservoir temperature (degC)
 T_i = isotherm temperature (degC)

A correction is also necessary for TOC as the gas can only adsorb onto kerogen. The simple linear relationship in Equation 7 has proven to adequately express that effect¹⁷.

$$V_{lc} = V_{lt} \cdot \frac{TOC_{lg}}{TOC_{iso}} \quad (7)$$

Where:

- V_{lc} = Langmuir volume at reservoir temperature corrected for TOC (scf/ton)
 TOC_{iso} = total organic carbon from isotherm (wt%)
 TOC_{lg} = total organic carbon from log (wt%)

A combination of the equations above leads to the following Langmuir isotherm that is used to calculate adsorbed gas.

$$gc = \frac{V_{lc} p}{(p + P_{lt})} \quad (8)$$

Track 3 of Figure 6 presents an adsorbed gas log calculated with Equation 8 that compares well with core. The core points represent canister desorption analyses. In this type of analysis a sample is retrieved from core, placed in a sealed tin, and sent to a laboratory where the quantity of desorbed gas is measured as the sample is heated. A correction is necessary to calculate the lost gas—gas liberated prior to isolating and sealing the sample. This type of analysis is not as useful for gas shale characterization as a Langmuir isotherm because there is potential for error in calculating lost gas, and it is not possible to differentiate free from adsorbed gas. The Langmuir isotherm is the preferred analysis. It is not affected by errors in lost gas estimation, it does not include potential additions from free gas, and it generates the inputs required to calculate adsorbed gas: Langmuir volume, Langmuir pressure, temperature, pressure, and TOC. The principal weakness with a Langmuir isotherm is that it measures the amount of gas the shale can hold, so it will overestimate gas volume if the shale is depleted.

Free Gas Quantification

Figure 8 presents gas content (adsorbed, free, and total) versus pressure for the gas shale depicted in the log examples (other than Figure 1). Several important features can be discerned from this figure: adsorption is more efficient at storing gas at low pressures, while free gas represents the dominant quantity of gas at higher pressures. The percentage of free gas in shale gas plays ranges from 15 to 80%², depending upon reservoir pressure, porosity and gas saturation. Thus, the quantification of free gas is also necessary to characterize gas shale.

The total and effective porosity plus gas saturation can be calculated for gas shale using a petrophysical interpretation program like ELAN. As with adsorbed gas, it is critical to have an accurate quantification of clay mineral content. This is especially important

for calculating accurate saturations that require an estimation of pore and bound water salinity for the gas shale. Water samples from gas shales are very scarce because most gas shales are generally at irreducible water saturation. Therefore, calibration to core analysis commonly provides the best means to estimate salinity. Figure 9 presents ELAN water saturation, total and effective porosity logs for a conventional and gas shale. Core results are also plotted in the figure.

Equations exist for the conversion of effective porosity, gas saturation, gas gravity, formation pressure and temperature into gas quantity at stock tank conditions²⁰. In order to facilitate direct comparison between free and adsorbed gas, the free gas is converted to scf/ton using Equation 9.

$$Gcfm = \frac{1}{B_g} \cdot (\phi_{eff} (1 - S_w)) \cdot \frac{\psi}{\rho_b} \quad (9)$$

Where:

- $Gcfm$ = free gas volume (scf/ton)
- B_g = gas formation volume factor (reservoir cf/scf)
- ϕ_{eff} = effective porosity (vol/vol)
- S_w = water saturation (vol/vol)
- ρ_b = bulk density (g/cm3)
- ψ = conversion constant (32.1052)

Figure 10 presents a total gas log for the conventional and gas shale. Track 3 shows both adsorbed and total gas in scf/ton. In addition, total gas in place is computed (BCF/section) for both adsorbed and total gas. This provides the operator with the ultimate potential of their shale gas reservoir, and it permits the future calculation of recovery efficiency.

Geochemical logging tools operate in cased holes. Combining existing open hole logs with a cased-hole geochemical log would allow the evaluation of the thousands of producing wells that penetrate potential gas shales.

Producibility

Permeability in tight gas shales is a key factor in stimulation design and production prediction. Two permeabilities need to be considered: matrix and system.

Matrix permeability of the shale rock is typically 10^{-4} to 10^{-8} mD. Matrix permeability can be accurately measured with core analysis, or it may be estimated via log evaluation if a local calibration can be developed.

System permeability is equivalent to matrix permeability plus the contribution of open fractures. Conventional logs are insensitive to fractures and cannot be used to estimate system permeability. The Fullbore Formation MicroImager* (FMI) is commonly run in gas shales to identify and map fractures that intersect the borehole. Fracture apertures can also be estimated²¹. These data are very useful in determining where to perforate the shale and predicting the azimuth of the fracture wings. Electrical imager data can provide a qualitative estimate of producibility, but they cannot provide a quantitative estimate of system permeability.

The preferred method for determining system permeability is pressure transient testing. A pressure buildup yields parameters

necessary to determine the productivity of the shale (reservoir pressure and system permeability) and examine the effectiveness of the stimulation treatment (fracture half-length and conductivity). Subsequent to this testing, excellent results have been achieved in evaluating shale, prior to stimulation. One such technique uses nitrogen or water injection followed by a falloff test. These techniques are applicable in reservoirs that will not flow prior to stimulation. In a well that has the potential to flow prior to stimulation, a conventional build up test after a nitrogen breakdown has been used successfully. Figure 11 presents a pressure derivative plot from a pressure buildup test performed on a gas shale. Note the relatively high system permeability due to the presence of open fractures.

A production history match can be performed using the ShaleGAS simulator²²⁻²⁶. It is a finite difference, dual-porosity reservoir simulator expressly developed for gas shales by Schlumberger Consulting Services. Unlike most oilfield simulators, it does include adsorbed gas in its calculations. The simulator inputs the core, log, and test data that have been described in the body of this report: Langmuir volume and pressure, TOC, porosity, gas saturation, pressure, temperature, gas gravity, system and matrix permeability. ShaleGAS also allows the input of natural fracture spacing and fracture permeability. This also permits the input of hydraulic fracture half-length and conductivity to predict the efficiency and economy of different stimulation designs. Figure 12 presents a cumulative production prediction for a gas shale well over a 30-year life.

CONCLUSIONS

This paper outlines a complete evaluation package for gas shale reservoirs. The individual components are:

- Log evaluation using triple combo and geochemical logs to quantify adsorbed and free gas. Geochemical logging is critical to the evaluation because it provides an accurate clay content independent of kerogen.
- Core analysis to measure the Langmuir isotherm. Generally, only one well need be sampled in a field or sub-basin.
- Pressure injection or build up testing to measure formation pressure and system permeability.
- ShaleGAS simulator to predict production and evaluate stimulation design. It is expressly designed to simulate gas shales and inputs log, core, and testing data.

REFERENCES

1. Hill, D.G. and Nelson, C.R.: "Gas Productive Fractured Shales: An Overview and Update," *GasTIPS* (Summer 2000).
2. Curtis, J.B.: "Fracture Shale-Gas Systems," *AAPG Bulletin* (2002) **86**, 1921.
3. Pollastro, R.M., Hill, R.J., Jarvie, D.M., and Henry, M.E.: "Assessing Undiscovered Resources of the Barnett-Paleozoic Total Petroleum System, Bend Arch-Fort Worth Basin Province, Texas," presented at AAPG Southwestern meeting held in Fort Worth, TX, March, 2003.
4. Bowker, K.: "Recent Developments of the Barnett Shale Play, Fort Worth Basin," presented at RMAG Petroleum Technology Transfer Council, Denver, CO, October 2002.
5. Gubelin, G.: "Improving Gas Recovery Factor in the Barnett Shale Through the Application of Reservoir Characterization and Simulation Answers," presented at Gas Shales: Production & Potential meeting held in Denver, CO, July 29-30, 2004.
6. Fritz, R.: "Bakken Shale and Austin Chalk," *AAPG Continuing Education Course Note* (1991) 33, 91.
7. Tissot, B.P. and Welte, D.H.: *Petroleum Formation and Occurrence*, 1978, Springer-Verlag, Berlin, 538 p.
8. Huang, W.H.: "Geochemical and Sedimentologic Problems of Uranium Deposits of Texas Gulf Coastal Plain," *AAPG Bulletin* (1978) **62**, 1049.
9. Passey, Q.R., Creaney, S., Kulla, J.B., Moretti, F.J., and Stroud, J.D.: "A Practical Model for Organic Richness from Porosity and Resistivity Logs," *AAPG Bulletin* (1990) **74**, 1777.
10. Campbell, R.L. Jr., and Truman, R.B.: "Formation Evaluation in the Devonian Shale," paper 15212 presented at SPE Unconventional Gas Technology Symposium held in Louisville, KY, May 18-21, 1986.
11. Herron, S.L. and Herron, M.M.: "Quantitative Lithology: An Application for Open and Cased Hole Spectroscopy," paper E presented at the 1996 SPWLA Annual Logging Symposium held in New Orleans, LA, June 16-19.
12. Quirein, J., Kimminau, S., LaVigne, J., Singer, J., and Wendel, F.: "A Coherent Framework for Developing and Applying Multiple Formation Evaluation Models," paper DD presented at the 1986 Annual SPWLA Logging Symposium, June 9-13.
13. Mayer, C. and Sibbit, A.: "GLOBAL. A New Approach to Computer-Processed Log Interpretation," paper 9341 presented at the 1980 SPE Annual Technical Conference and Exhibition.
14. Cannon, D.E.: "Use of Spectral Data (NGT, HNGS, ECS, RST, GST) in ELAN," 1998 Schlumberger Letter Report.
15. Herron, S.L., and Herron, M.M.: "Application of Nuclear Spectroscopy Logs to the Derivation of Formation Matrix Density," paper JJ presented at the SPWLA Annual Logging Symposium held in Dallas, TX, June 4-7, 2000.
16. Herron, S.L. and Le Tendre, L.: "Wireline Source-Rock Evaluation in the Paris Basin," *AAPG Stud. Geol.* (1990) **30**, 57.
17. Langmuir, I.: "Adsorption of Gases on Glass, Mica, and Platinum," *J. Am. Chem. Soc.* (1918) **40**, 1361.
18. Hawkins, J.M., Schraufnagel, R.A., and Olszewski, A.J.: "Estimating Coalbed Gas Content and Sorption Isotherm Using Well Log Data," paper SPE 24905 presented at 1992 SPE Annual Technical Conference and Exhibition held in Washington, DC, Oct. 4-7.
19. Zuber, M.D., Frantz, J.H. Jr., and Gatens, J.M. III: "Reservoir Characterization and Production Forecasting for Antrim Shale Wells: An Integrated Reservoir Analysis Methodology," paper SPE 28606 presented at 1994 SPE Annual Technical Conference and Exhibition held in New Orleans, LA, Sept. 25-28.
20. Craft, B.C. and Hawkins, M.F.: *Applied Petroleum Reservoir Engineering*, 1991, Prentice-Hall, NJ.
21. Luthi, S.M. and Souhaite, P.: "Fracture Apertures from Electrical Borehole Scans," *Geophysics* (1990) **55**, 821.
22. Frantz, J.H., Gatens, J.M. III, and Hopkins, S.A.: "Using a Multilayer Reservoir Model To Describe a Hydraulically Fractured, Low-Permeability Shale Reservoir," paper SPE 24885 presented at the 1992 SPE Annual Technical Conference and Exhibition held in Washington, DC, Oct. 4-7.
23. Frantz, J. H. Jr., Fairchild, N. R., Dube, H. G., Campbell, S. M., Christiansen, G. E., and Olszewski, A. J.: "Evaluating Reservoir Production Mechanisms and Hydraulic Fracture Geometry in the Lewis Shale, San Juan Basin," paper SPE 56552 presented at the 1999 Annual Technical Conference and Exhibition, Houston, October 3-6
24. Frantz, Jr., J. H., Hopkins, C. W., Zuber, M. D., Gatens, J. M. III, Voneiff, G. W., Jochen, J. E., and Yeager, D. L.: Antrim Shale Development Technology Project, GRI Final Report, GRI-96/0389, November 1996.
25. Frantz, Jr., J. H. and Lancaster, D. E.: "Research Results from the Ashland Exploration, Inc. FMC 80 (COOP 2) Well, Pike County, KY," GRI-94/0258, April 1993.
26. Gatens, J. M. III, Hopkins, C. W., and Frantz, J. H.: "The Effect of Permeability Distribution on Reservoir Performance and Stimulation Potential," *Devonian Gas Shales Technology Review* (March 1992) **7**, no. 3, 2437.

TABLES

Bulk density	1.0 – 1.1 g/cm ³
U	0.18 – 0.24
Neutron porosity	50 – 65 pu
Gamma ray activity	500 - 4000 gAPI
Sonic slowness	160 μs/ft

Table 1. Petrophysical properties of kerogen.

Stage	Type of Kerogen		
	I	II	III
Diagenesis	1.25	1.34	1.48
End of catagenesis	1.20	1.19	1.18

Table 2. Conversion factors for kerogen to TOC.
 (Diagenesis - transformation of sediments into rocks due to compaction and microbial activity. Organic matter consists primarily of kerogen by end of this phase. Catagenesis - temperature and pressure increases from burial lead to the thermal degradation of kerogen and generation of hydrocarbons⁷.)

FIGURES

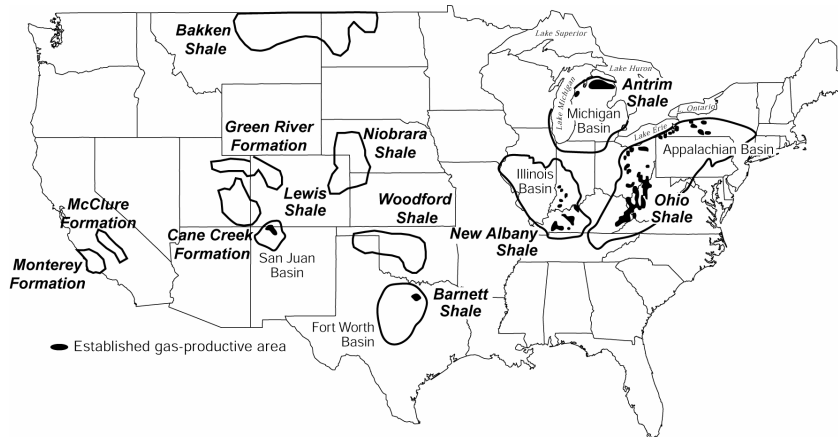


Figure 1. Distribution of Gas Shale Reservoirs in the United States¹.

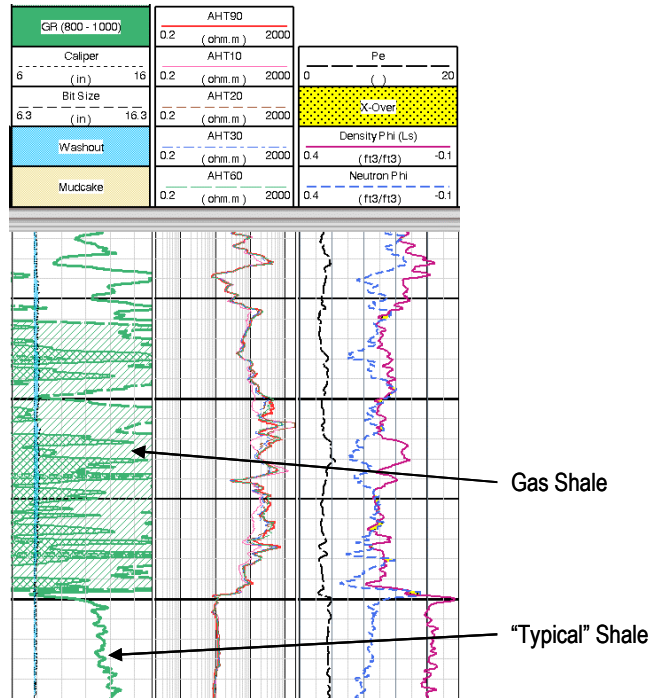


Figure 2. Log of conventional and gas shale. The conventional is the Sylvan Formation; the gas shale is the Woodford. (Each dark horizontal line represents 10 feet.)

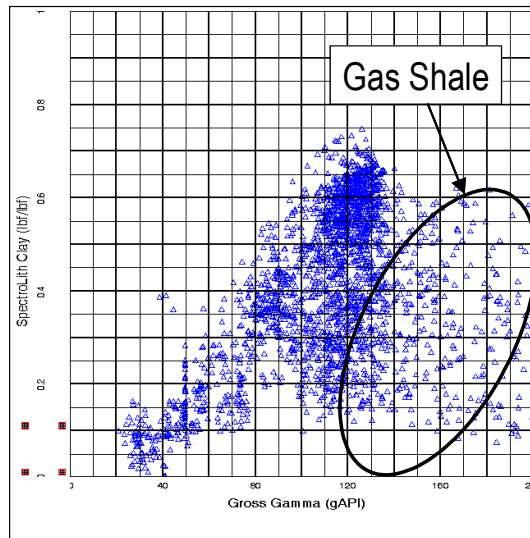


Figure 3. Cross plot of gross gamma vs. SpectroLith clay content. Gas shale is apparent due to high gamma ray activity that is not a function of clay content.

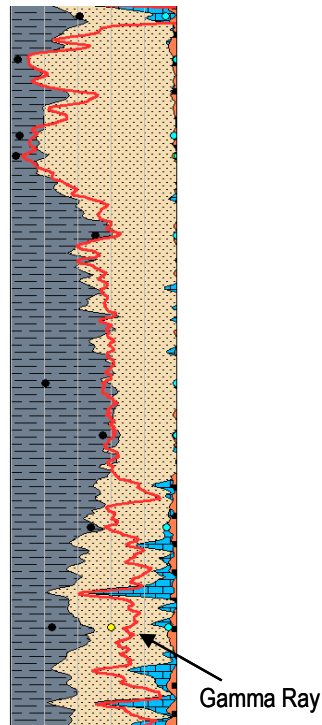


Figure 4. SpectroLith and gross gamma ray log of conventional shale overlying gas shale. Gas shale has lower clay content plus pyrite and carbonate. XRD core analyses are also plotted. Total interval is about 150 feet.

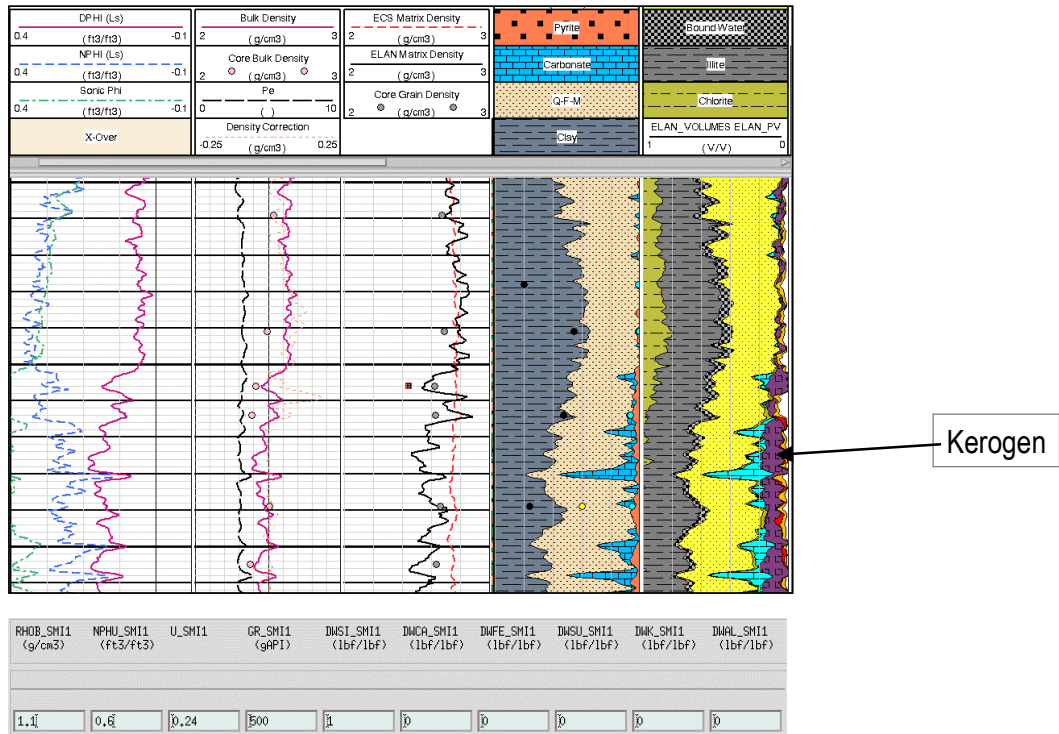


Figure 5. Conventional log analyses, SpectroLith, and ELANPlus interpretation of conventional and underlying gas shale. Kerogen is highlighted in ELANPlus track. Third track depicts apparent grain density calculated by SpectroLith (red dash), apparent grain density calculated by ELANPlus (black solid), and core analyses. Note that SpectroLith grain density is inaccurate in the gas shale. (Each dark horizontal line represents 10 feet.) Chart on bottom lists the kerogen parameters entered into the ELANPlus solve model.

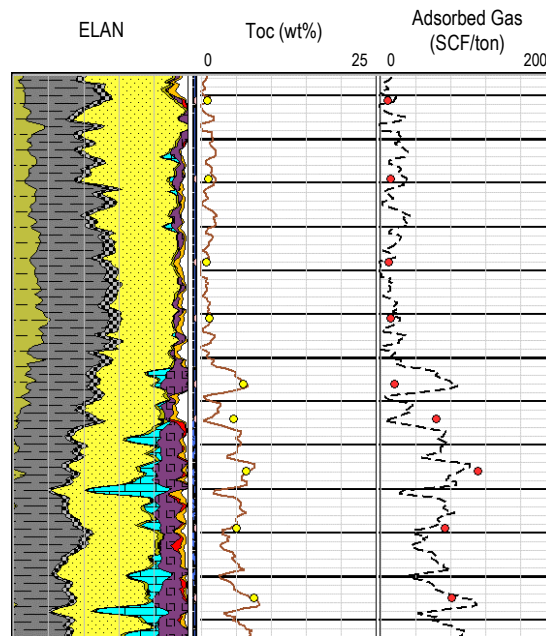


Figure 6. SpectroLith, TOC, and adsorbed gas log of conventional and gas shale. Note that in track 2 the core and log TOC compare well. The desorption gas core analyses in track 3 also compare favorably with adsorbed gas log. (Each dark horizontal line represents 10 feet.)

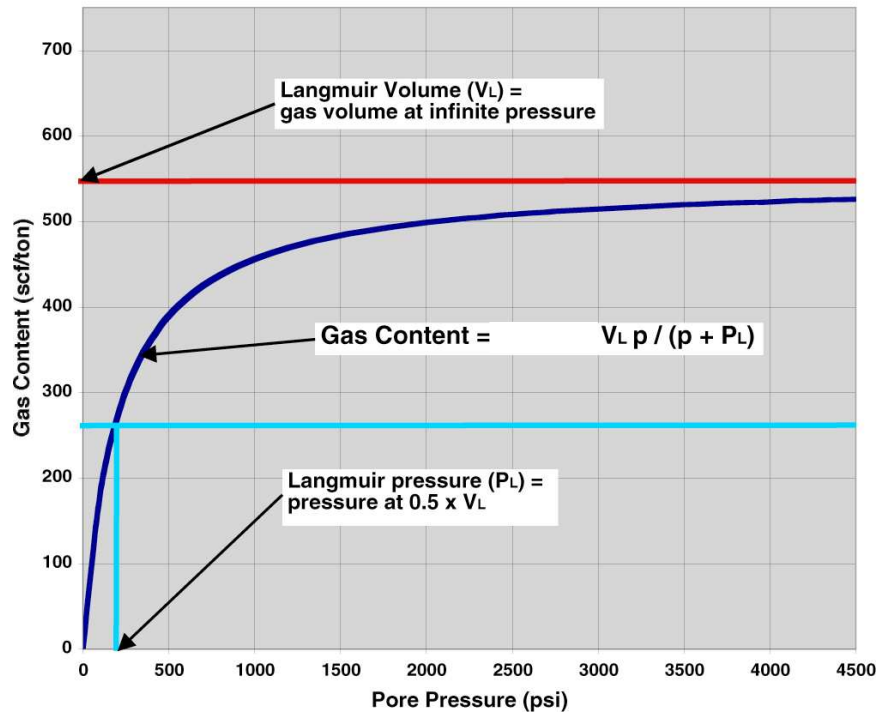


Figure 7. Langmuir isotherm.

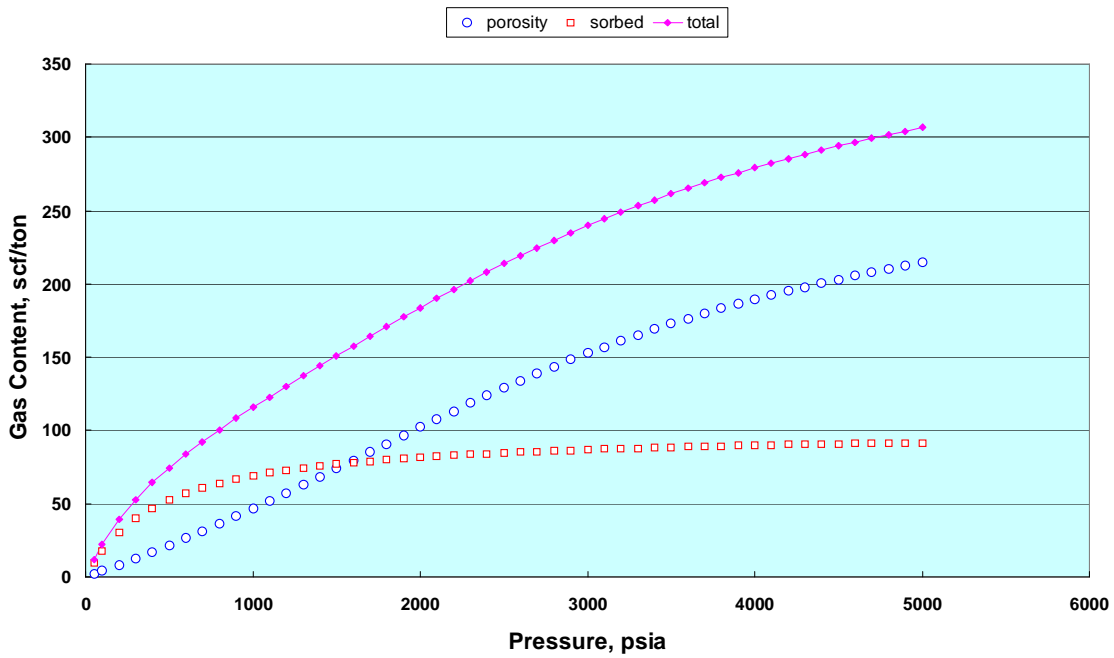


Figure 8. Gas content in scf/ton versus pressure for gas shale. The red dots indicate adsorbed gas content, the blue is free gas in the pore spaces, and the pink line is the total gas. Sorption is a very efficient mode of gas storage at low pressures; however, as pressures increase free gas eventually represents the majority of the gas. The crossover is a function of effective porosity, water saturation, and pressure.

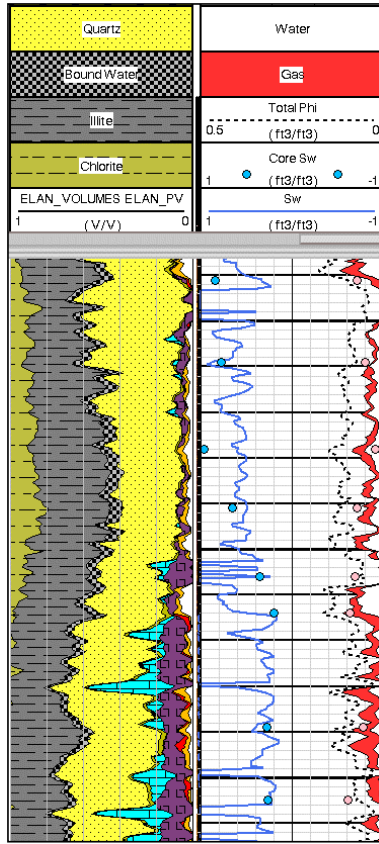


Figure 9. Log showing ELANPlus volumes and free gas for conventional and gas shales. Track 2 shows water saturation (blue), total porosity (black dash), effective porosity, gas-filled porosity (red shading), and water-filled porosity (white shading). (Each dark horizontal line represents 10 feet.)

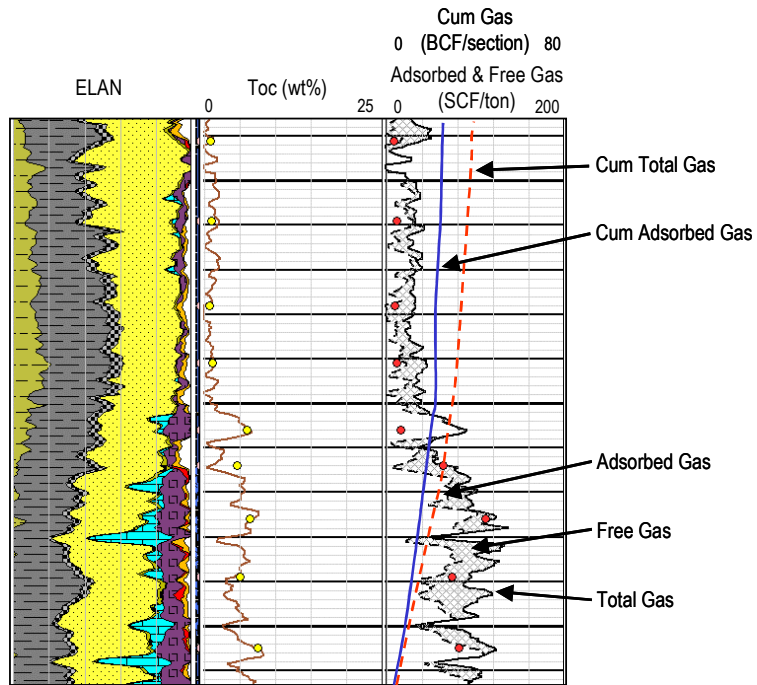


Figure 10. Total gas log of conventional and gas shale. Track1 shows ELANPlus volumes and track 2 depicts TOC. Track 3 shows adsorbed and total gas in scf/ton. The difference, shaded in gray, is the free gas. Track 3 also depicts cumulative adsorbed and total gas in BCF/section. (Each dark horizontal line represents 10 feet.)

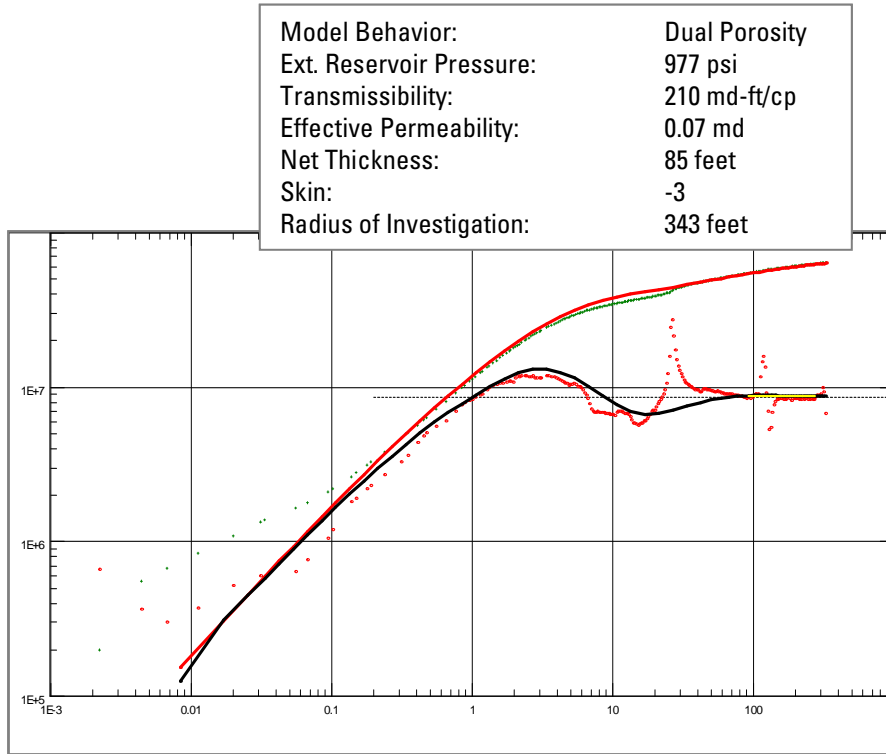


Figure 11. Pressure derivative plot from pressure buildup test performed on gas shale. Results of analysis are listed at top. The relatively high effective permeability is probably due to open natural fractures within the shale.

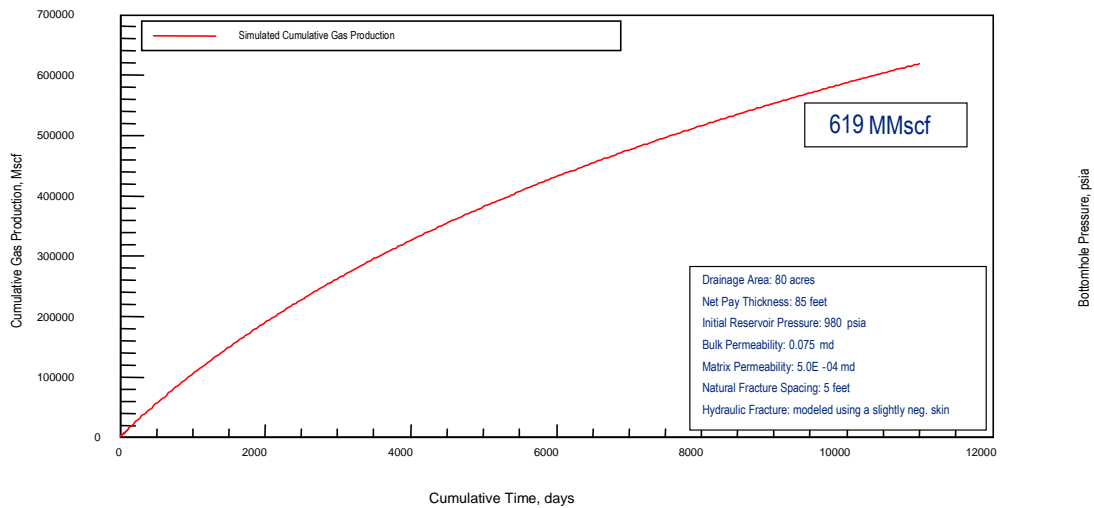


Figure 12. Cumulative production prediction from ShaleGAS simulator. Gas production continues at a fairly rate throughout the 30 years this simulation represents. This response is typical for gas shale reservoirs.